Environ. Chem. **2014**, *11*, 257-267
doi:10.1071/EN13191_AC

Supplementary material

Nanoparticle core properties affect attachment of macromolecule-coated nanoparticles to silica surfaces

Ernest M. Hotze[A,B], *Stacey M. Louie*[A,B], *Shihong Lin*[A,C], *Mark R. Wiesner*[A,C] and *Gregory V. Lowry*[A,B,D]

[A]Center for Environmental Implications of NanoTechnology (CEINT), PO Box 90287, Duke University, Durham, NC 27708-0287, USA.

[B]Department of Civil and Environmental Engineering, Carnegie Mellon University, Pittsburgh, PA, 15213, USA.

[C]Department of Civil and Environmental Engineering, Duke University, 121 Hudson Hall, Box 90287, Durham, NC 27708-0287.

[D]Corresponding author. Email: glowry@andrew.cmu.edu

Synthesis of citrate-stabilised silver nanoparticles

Silver nitrate was purchased from Sigma–Aldrich. Sodium citrate dihydrate was acquired from Fisher Scientific. Citrate-stabilised silver was formed in a round-bottom flask equipped with a condenser as follows: 1 L of 1-mM silver nitrate in water was brought to reflux while stirring. Five millilitres of 1-M sodium citrate was added all at once, and reflux and stirring were continued for 30 min. The yellow suspension was removed from heat, and stirring was continued until cool. The citrate-stabilised silver nanoparticles were filtered through a 0.2-μm filter (Corning) and then stored at 4 °C away from light until further use.[1]

Saturation adsorbed mass of macromolecules on nanoparticles

Previously published values of saturated or plateau adsorbed mass for the macromolecule and nanoparticle types used in this study are provided in Table S1 for comparison to those obtained here. The adsorbed masses determined in this study were in some cases lower than the saturated amount expected from the reported adsorption isotherms, but we note that differences in the particle properties (e.g. size, aggregation state, shape, crystallinity), polymer molecular weight and polydispersity, and suspension conditions used (ionic strength, pH) can all contribute to differences in adsorption. In this study, the adsorption was performed in 1 mM $NaHCO_3$ at pH 7.

Table S1. Reported saturation adsorbed mass for materials used in this study

Reported saturation adsorbed mass values are approximated from the plateau region of the adsorption isotherm when not explicitly reported. When originally reported in units of milligrams per gram, values are converted to milligrams per square metre using the reported specific surface area or that calculated from the material density and reported particle size. For the HA on Ag-cit, total mass of HA was estimated from the reported mass (as carbon) by estimating ~50 wt% carbon.

Coating type	NP type	Adsorbed mass in this study (mg m^{-2})	Reported saturation adsorbed mass (mg m^{-2})	Material properties and suspension conditions used in referenced study
HA	TiO_2	0.18	0.3–0.65[2]	pH 7
			0.3[3]	pH not reported
HA	Ag-cit	1.97	4[4]	Suwannee River humic acid; pH 7
HA	C_{60}	5.38	0.5–1[5]	Peat humic acid; pH 7
			15.8[6]	pH 3.2; I = 10 mM
PAA	TiO_2	0.04	0.3–0.6[7]	MW = 10 000 or 120 000; pH 3 or 9.5
			0.1–0.5[8]	MW = 4000; pH 4.5 or 9.8
			0.2[9]	MW = 60 000 ; ‘natural pH’, 1 mM NaCl
PAA	Ag-cit	b.d.	n/a	
PAA	C60	b.d.	n/a	
BSA	TiO_2	0.27	2.2[10]	pH 5; I = 154 mM
			1.7[11]	pH 7.3; I = 10 mM
BSA	Ag-cit	2.9	8[12]	Ag (without citrate); pH 7; I = 10 mM
BSA	C60	b.d.	n/a	

Effect of particle size on electrophoretic mobility

When the ratio of particle size to Debye length (κa, where κ is the Debye parameter and a is the particle radius) lies within the limits of the Hückel and Smoluchowski approximations (i.e. $1 < \kappa a < 300$), changes in particle size or aggregation can affect the electrophoretic mobility according to the Henry function ($f(\kappa a)$), which can be approximated as follows[13]:

$$f(\kappa a) = \frac{16 + 18\kappa a + 3(\kappa a)^2}{16 + 18\kappa a + 2(\kappa a)^2} \quad \text{(S1)}$$

The electrophoretic mobility (μ or EPM) is

$$\mu = \frac{2\varepsilon\varepsilon_0\zeta}{3\eta} f(\kappa a) \quad \text{(S2)}$$

where ε is the dielectric constant of the dispersion medium, ε_0 is the permittivity of vacuum, η is the viscosity of the dispersion medium and ζ is the zeta potential of the particle. Assuming the surface charge and ζ of the hard particle surface remain unchanged upon aggregation or disaggregation, the change in the magnitude of the electrophoretic mobility, $|\mu|$ due solely to aggregation state (without considering the charged coating) will be proportional to the change in $f(\kappa a)$. The calculated $f(\kappa a)$ using the number-averaged hydrodynamic size by dynamic light scattering is reported in Table S2 and compared to the measured change in $|\mu|$ for the coated nanoparticles. The size change is insufficient to explain the measured change in $|\mu|$ except for BSA-coated TiO_2, suggesting that the change in $|\mu|$ is primarily attributable to the charge and hydrodynamic properties of the adsorbed coating rather than to changes in nanoparticle aggregation state.

Table S2. Effect of particle size on electrophoretic mobility

Number average particle hydrodynamic diameter measured by dynamic light scattering

Particle type	Particle hydrodynamic diameter (nm)	Measured particle EPM (μ) at 1-mM ionic strength ($\mu m\ cm\ V^{-1}\ s^{-1}$)	$f(ka)$ at 1-mM ionic strength	Change in $\lvert\mu\rvert$ relative to bare particle $\lvert\mu\rvert$ due to change in particle size (from $f(\kappa a)$)	Measured change in $\lvert\mu\rvert$ relative to bare particle $\lvert\mu\rvert$
TiO_2	132	–1.94	1.19		
Ag-Citrate	99	–3.74	1.16		
C_{60}	204	–0.83	1.26		
TiO_2 + HA	103	–2.84	1.17	–2%	+46%
Ag + HA	165	–2.17	1.23	+6%	–42%
C_{60} + HA	50	–2.01	1.09	–14%	+142%
TiO_2 + PAA	183	–2.70	1.19	+0.1%	+39%
Ag + PAA	228	–1.37	1.28	+10%	–63%
C_{60} + PAA	87	–1.75	1.15	–9%	+111%
TiO_2 + BSA	439	–2.17	1.36	+14%	+12%
Ag + BSA	58	–1.82	1.10	–5%	–51%
C_{60} + BSA	108	–1.41	1.18	–7%	+70%

Macromolecule molecular weight distributions by size exclusion chromatography with multi-angle laser light scattering (SEC-MALLS)

Molecular weight distributions for the macromolecules used in this study were determined by SEC-MALLS. Concentration (by refractive index) and the simultaneously determined weight-average molecular weight (by MALLS) are plotted against the elution time. HA exhibits a broad peak, indicating its high polydispersity; the weight-average molecular weight is 60 000 g mol^{-1} (Fig. S1). BSA consists primarily of monomers eluting at ~13.6 min, as well as a smaller concentration of BSA dimers eluting at ~12 min (Fig. S2).

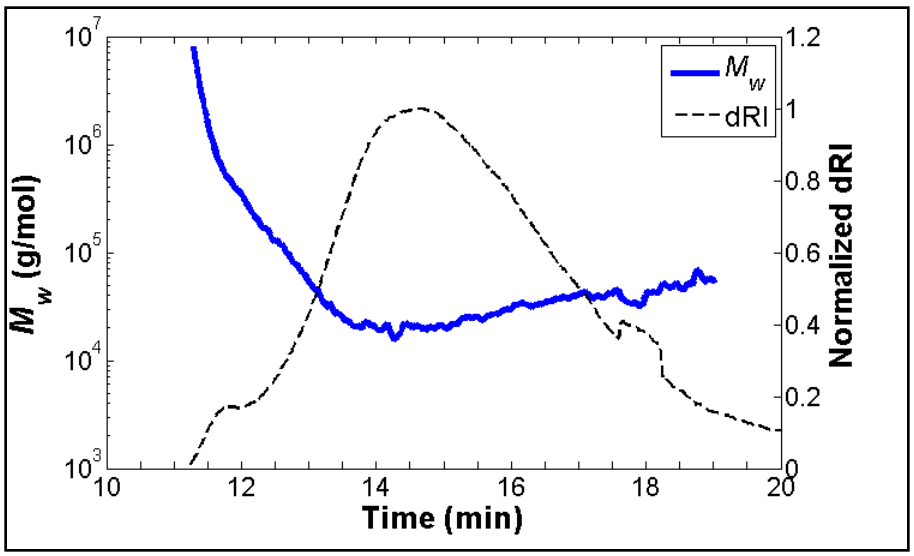

Fig. S1. SEC-MALLS elution profile of humic acid used in this study. The dashed curve indicates the refractive index peaks of humic acid eluting from the SEC column. The blue curve is the simultaneous estimate of weight-average molecular weight, M_w, based on multi-angle laser light scattering measurements.

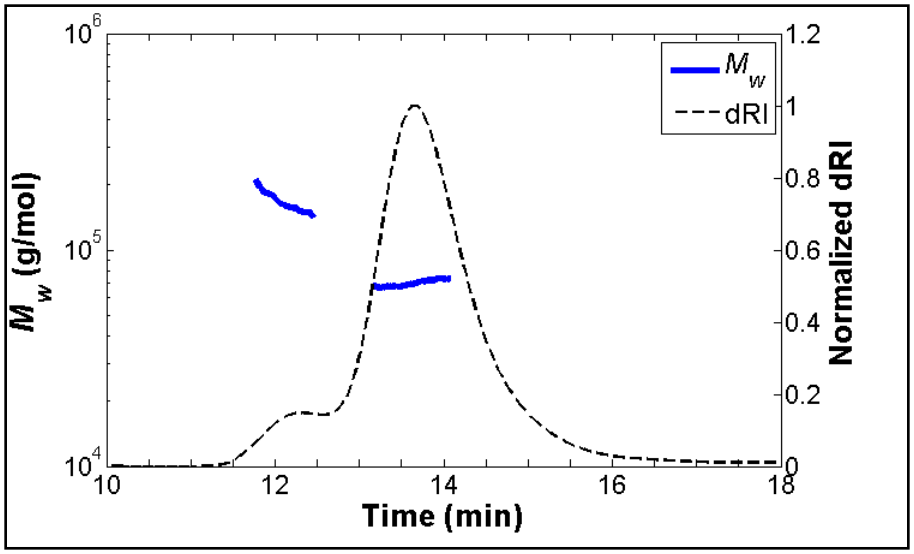

Fig. S2. SEC-MALLS elution profile of bovine serum albumin used in this study. The dashed curve indicates the refractive index peaks of bovine serum albumin eluting from the SEC column. The blue curve is the simultaneous estimate of weight-average molecular weight, M_w, based on multi-angle laser light scattering measurements.

Soft particle electrokinetic model

The coating properties are obtained by applying a soft particle electrokinetic model to fit electrophoretic mobility data for the bare and coated particles over a range of ionic strengths. Three coating parameters are obtained: layer thickness (d), volume charge density (N) and permeability or softness (λ^{-1}).

The model follows the formalism introduced by Ohshima[14] and describes the coated particle system as follows. A hard (impermeable) particle core with radius (a) and surface charge density (σ) is coated with a polymer or polyelectrolyte with unit charge (Z). The bulk solvent has relative permittivity (ε_{rr}) and viscosity (η), and contains $i = 1,\ldots, N_{el}$ species of mobile electrolytes, with unit charge (z_i), molar concentration (c_i) or number concentration (n_i) and ionic strength (I) (or Debye parameter κ).

The governing fundamental equations are the Navier–Stokes and continuity equations for incompressible fluid flow around the particle, with the potential profile defined by the Poisson–Boltzmann equation.[14–16] The flow equations for the fluid and mobile electrolyte are as follows:

$$\eta\nabla\times\nabla\times\vec{u}(\vec{r})+\nabla p(\vec{r})-\sum_{i=1}^{N_{el}}\delta\mu_i(\vec{r})\nabla c_i^{(0)}(\vec{r})+\rho_{el}^{(0)}(\vec{r})\nabla\psi^{(0)}(\vec{r})+\nabla(\rho_{el}^{(0)}(\vec{r})\delta\psi(\vec{r}))+k(\vec{r})\vec{u}(\vec{r})=\vec{0} \quad \text{(S3)}$$

$$\nabla\left\{c_i^{(0)}(\vec{r})\vec{u}(\vec{r})-\frac{1}{\overline{\lambda}_i}c_i^{(0)}(\vec{r})\nabla\delta\mu_i(\vec{r})\right\}=\vec{0} \text{ where } i=1,\ldots,N_{el} \quad \text{(S4)}$$

where $\vec{u}(\vec{r})$ is the liquid velocity at radial position $\vec{r}$, p is the pressure, ψ is the electric potential, N_{el} is the mobile electrolyte charge density, k is the friction coefficient for the polyelectrolyte layer, $\overline{\lambda}_i$ is the drag coefficient of the ith mobile ion and μ_i is the electrochemical potential of the ith mobile ion. The superscript (0) denotes equilibrium conditions (e.g. counter-ion distribution in the absence of an electric field) and δ denotes perturbations from equilibrium due to application of the electric field (polarisation and relaxation effects). The equilibrium potential profile $\psi^{(0)}$ is given by the Poisson–Boltzmann equation, and the drag coefficient $\overline{\lambda}_i = |z_i|eF/\lambda_i^0$, where e is the elementary charge, F is Faraday's constant and λ_i^0 is the limiting conductivity (5.01 mS m^2 mol^{-1} for Na^+ and 7.63 mS m^2 mol^{-1} for Cl^-). Boundary conditions for the Poisson–Boltzmann equation are specified to be zero potential far from the particle, and either (1) constant potential or (2) constant charge (establishing the slope of the potential profile) at the particle surface. For the flow equations, fluid velocity is zero at the hard particle surface and is expressed in terms of the electrophoretic mobility far from the particle surface.

Analytical solutions (which require assumptions on particle size, particle surface charge, coating thickness, homogeneity of the coating segment distribution, and polarisation or relaxation effects) have been obtained by Ohshima.[14,17] Because charged nanoparticles with potentially high charge density are used in this study, an 'exact' numerical model is required. Here, we used the MPEK program[16] provided by Dr Reghan Hill but maintain the assumption that the coating has homogeneous charge and segment distribution. Other numerical approaches are also available.[15,18]

The experimental electrophoretic mobility data are fitted using an iterative least-squares method to obtain layer parameters. Uncertainty or polydispersity in the bare particle size distribution are expected to affect electrophoretic mobility by at most ~15% according to the Henry function (Table S2), and model fitting has been shown to be relatively insensitive to particle polydispersity.[19] However, other sources of uncertainty exist. Adsorbed layers on the particles may not be homogeneous, violating assumptions taken when using the model. Non-uniformity of the polymer segment distribution, e.g. due to high surface curvature of nanoparticles, can be important.[20] Although segment density profiles can be incorporated into numerical electrokinetic models,[15,16] this would require an additional fitting parameter. Here, three parameters (layer thickness, charge density and permeability) were obtained together, as has been shown previously.[19,21,22] Statistical uncertainty in the three-parameter model can be significant, so a sensitivity analysis was performed as described by Louie et al.[23]

Sensitivity analysis of fitted layer thicknesses

The sensitivity of the electrokinetic model to layer thickness was assessed for each fitted parameter set to determine the confidence in the model fit, following the method presented by Brun et al.[24] and applied to the electrokinetic model by Louie et al.[23] The mean-square average (δ_d^{msqr}) of the sensitivity of the electrophoretic mobility to layer thickness is computed over the range of data (ionic strengths) measured, using Eqn S5. The model is represented by outputs (electrophoretic mobility) η_i where $i = (1, 2, \ldots, n)$ for n observations (ionic strengths), and the best fit parameter set is θ_j where j represents the parameter of interest (e.g. layer thickness).

$$\delta_j^{msqr} = \sqrt{\frac{1}{n}\sum_{i=1}^{n} s_{ij}^2} \qquad \text{(S5)}$$

The sensitivity at each data point (s_{ij}) is calculated as follows:

$$s_{ij} = \upsilon_{ij}\frac{\Delta\theta_j}{SC_i} \qquad \text{(S6)}$$

$$\upsilon_{ij} = \left.\frac{\partial \eta_i(\theta_j)}{\partial \theta_j}\right|_{\boldsymbol{\theta}=\boldsymbol{\theta_0}} \quad \text{(S7)}$$

where v_{ij} is the derivative of the modelled electrophoretic mobility with respect to parameter j, taken at the best fit parameter set θ_0. Here, the derivative is computed using a linear approximation between $\eta_i(\theta_{j0})$ and $\eta_i(1.1\theta_{j0})$, holding the other two parameters at their best fit values. $\Delta\theta_j$ and SC_i are scaling factors on the parameter θ and the electrophoretic mobility respectively. Values of $\Delta\theta_j$ = 1 nm and $SC_i = |\eta_i(\theta_0)|$ are chosen for consistency in comparison against results reported in Louie et al.[23] The sensitivity indices calculated for each system are reported in Table S3. Sensitivity indices were shown to be a reasonable surrogate to assess identifiability of layer thickness for this model.

Table S3. Sensitivity indices for fitted layer thickness of coated NP systems

Particle type	δ_d^{msqr}
TiO_2 + HA	0.02
Ag + HA	0.004
C_{60} + HA	0.02
TiO_2 + PAA	0.03
Ag + PAA	0.04
C_{60} + PAA	0.03
TiO_2 + BSA	0.03
Ag + BSA	0.005
C_{60} + BSA	0.03

For the electrokinetic model, δ_d^{msqr} values lower than 0.009 indicate poor sensitivity of the model (non-identifiable layer thickness), whereas cases with identifiable layer thicknesses generally have δ_d^{msqr} values higher than ~0.06.[23] Therefore, confidence in the estimates for Ag coated with HA and BSA is poor, and the layer thicknesses are likely overestimated. Conditional likelihood regions were also plotted (not shown) to more rigorously assess the extent of the uncertainty in layer thickness at 80 and 95% confidence intervals (based on the standard deviation in the experimental electrophoretic mobility data). These plots also indicate that the layer thickness estimates using this method are unreliable for the coated Ag and C_{60} particles, with uncertainty in layer thickness only bounded for the coated TiO_2 particles.

Correlation equation for single-collector contact efficiency (η_0)

The single-collector contact efficiency equation by Tufenkji and Elimelech was used to calculate η_0 for the attachment efficiency equation[25]:

$$\eta_0 = 2.4A_s^{1/3}N_R^{-0.081}N_{Pe}^{-0.715}N_{vdW}^{0.052} + 0.55A_sN_R^{1.675}N_A^{0.125} + 0.22N_R^{-0.24}N_G^{1.11}N_{vdW}^{0.053} \quad \text{(S8)}$$

where A_s is a porosity-dependent parameter, N_R is the aspect ratio, N_{Pe} is the Peclet number, N_{vdW} is the van der Waals number, N_A is the attraction number and N_G is the gravity number. The reader is referred to the work by Tufenkji and Elimelech for definitions of these dimensionless parameters.[25]

Semi-empirical correlation of attachment efficiency (α)

Briefly, Phenrat et al.[21] derived a dimensionless number using the Buckingham-Π approach based on an analysis of several sets of attachment efficiency data for coated nanoparticles, N_{LEK}:

$$N_{LEK} = \frac{d_p d_M^2 u_s \Gamma N_a \rho_p}{\mu M_W} \quad \text{(S9)}$$

where d_p is the particle diameter, d_M is the adsorbed layer thickness (Table 1), u_s is the porewater velocity in the column, Γ is the surface concentration of adsorbed macromolecule (Table 1), N_a is Avagadro's number, ρ_p is coating density, μ is viscosity and M_W is the coating molecular weight (Table 1). N_{LEK} represents both electrosteric repulsions and decreased frictional forces that arise when coatings are on the surface of a particle. The corresponding empirical equation including this dimensionless number is a predicted attachment value (α_{pre})[21]:

$$\alpha_{pre} = 10^{-1.35}N_{LO}^{0.39}N_{E1}^{-1.17}N_{LEK}^{-0.10} \quad \text{(S10)}$$

We emphasise that the utility of this approach was likely hindered by the poor certainty in layer thickness estimates obtained by fitting the soft particle electrokinetic model and the lack of alternative methods to obtain layer thickness, resulting in a poor ability to quantify steric or electrosteric interactions.

Particle size distributions by dynamic light scattering (DLS)

Uncoated and coated particle DLS measurements were taken on a Malvern Zetasizer Nano ZS (Malvern, Southborough, MA) and fitted using a non-negative least-squares (NNLS) algorithm to obtain size distributions. Size distributions for TiO_2, Ag and C_{60} are respectively shown in Figs S3, S4 and S5.

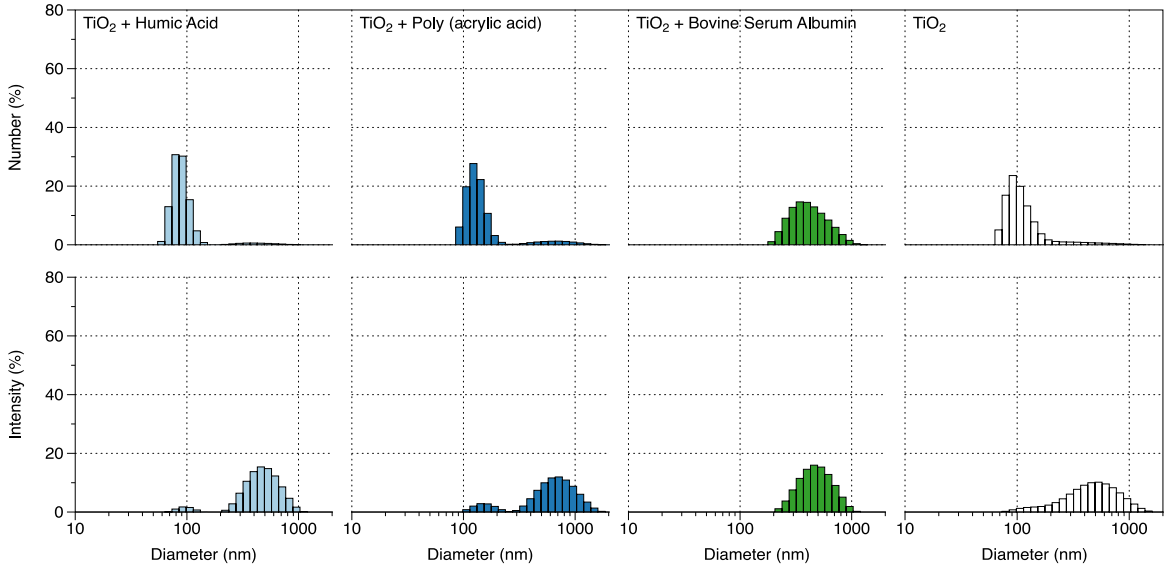

Fig. S3. Dynamic light scattering measurements of size distribution for uncoated TiO_2 particles, and those coated with humic acid, poly(acrylic acid) and bovine serum albumin. Both number (top) and intensity (bottom) distributions are given. Particle diameter was determined by fitting multiple exponentials to the correlation function to obtain the distribution of particle sizes using a non-negative least-squares algorithm.

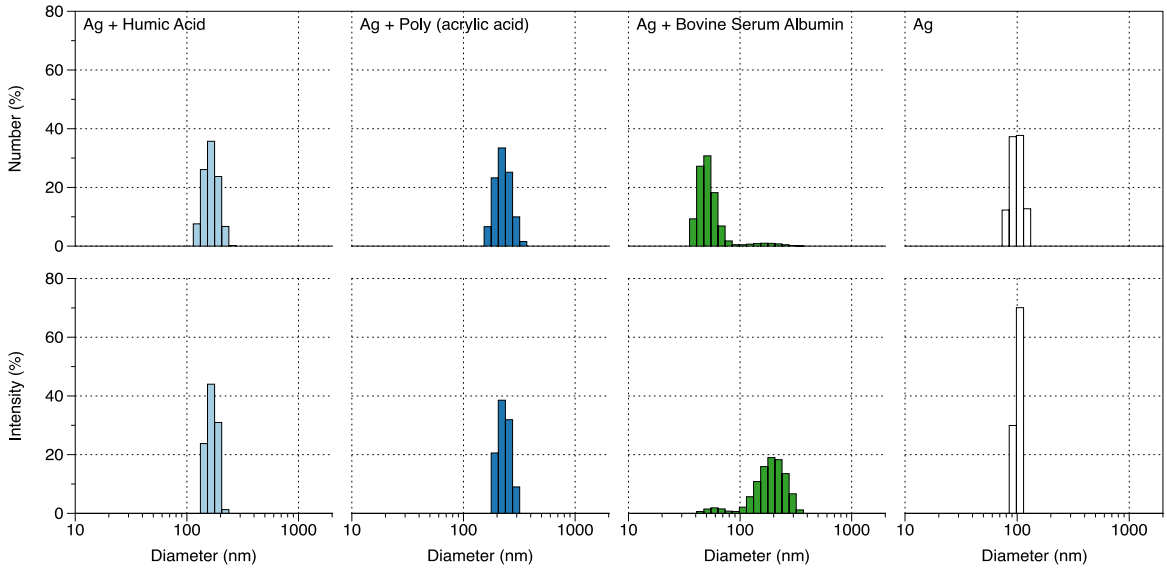

Fig. S4. Dynamic light scattering measurements of size distribution for Ag-citrate particles, and those coated with humic acid, poly(acrylic acid) and bovine serum albumin. Both number (top) and intensity (bottom) distributions are given. Particle diameter was determined by fitting multiple exponentials to the correlation function to obtain the distribution of particle sizes using a non-negative least-squares algorithm.

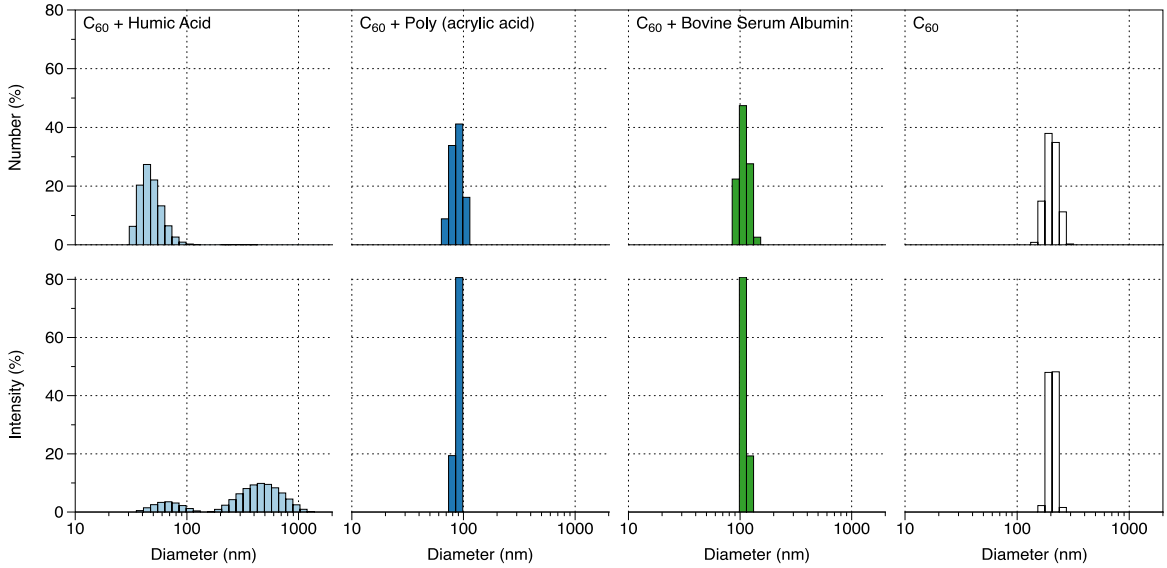

Fig. S5. Dynamic light scattering measurements of size distribution for uncoated C_{60} particles, and those coated with humic acid, poly(acrylic acid) and bovine serum albumin. Both number (top) and intensity (bottom) distributions are given. Particle diameter was determined by fitting multiple exponentials to the correlation function to obtain the distribution of particle sizes using a non-negative least-squares algorithm.

Consideration of attachment efficiency correlations

Correlations were attempted between attachment efficiency and individual or multiple particle and adsorbed layer properties that were measured in this study. Specifically, α_{exp} is plotted against the coated particle number-average diameter (Fig. S6), electrophoretic mobility (Fig. S7), surface layer thickness estimated using the soft particle electrokinetic model (Fig. S8) and surface layer concentration (Fig. S9). Lines of best fit were determined for each case; poor correlations show that no single property assessed here could explain the attachment efficiency of the coated particles. The multi-parameter semi-empirical correlation[21] described above was also considered: attachment efficiencies predicted using this correlation are plotted against experimental attachment efficiencies (Fig. S10). This correlation failed to predict the experimental data and consistently underestimated particle attachment efficiency for the samples assessed in this study.

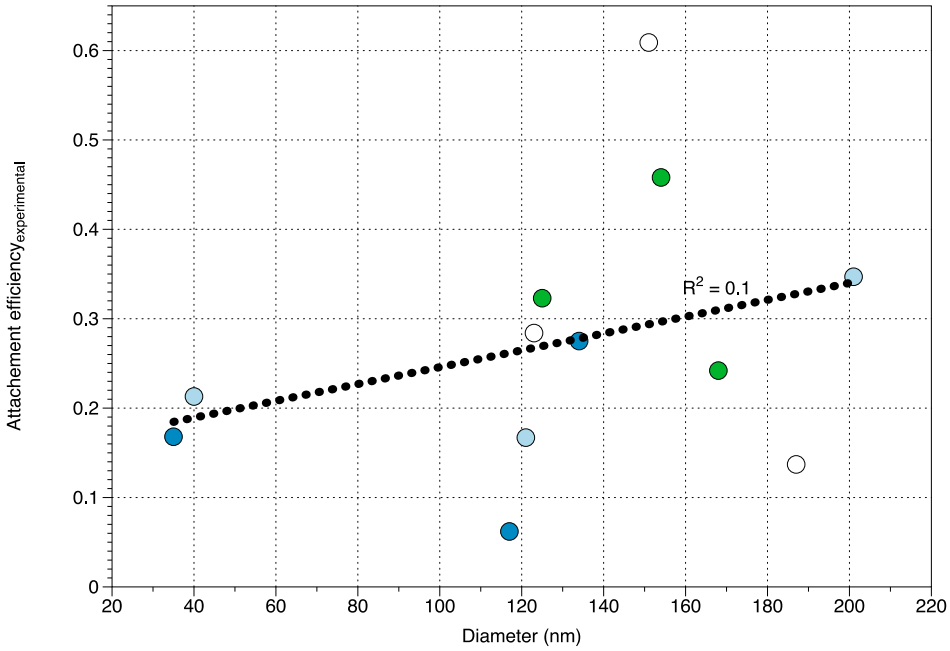

Fig. S6. Comparison of attachment efficiency calculated from column experiments with number-averaged diameter given by dynamic light scattering measurements. R^2 value of 0.1 indicates a low correlation. Colours represent bare (white), humic acid- (light blue), PAA- (dark blue) and BSA-coated (green) particles.

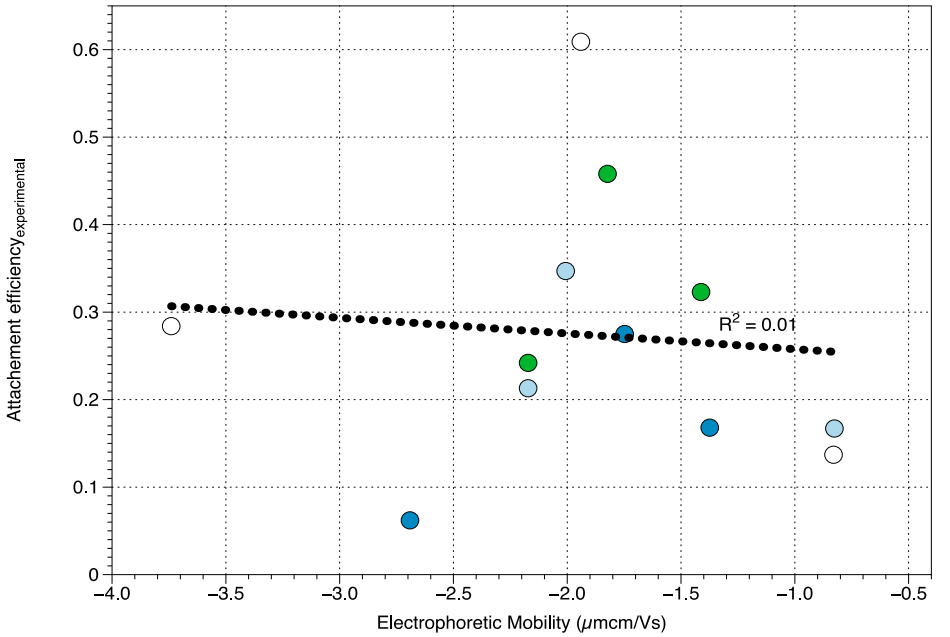

Fig. S7. Comparison of attachment efficiency calculated from column experiments with electrophoretic mobility. R^2 value of 0.01 indicates a very low correlation. Colours represent bare (white), humic acid- (light blue), PAA- (dark blue) and BSA-coated (green) particles.

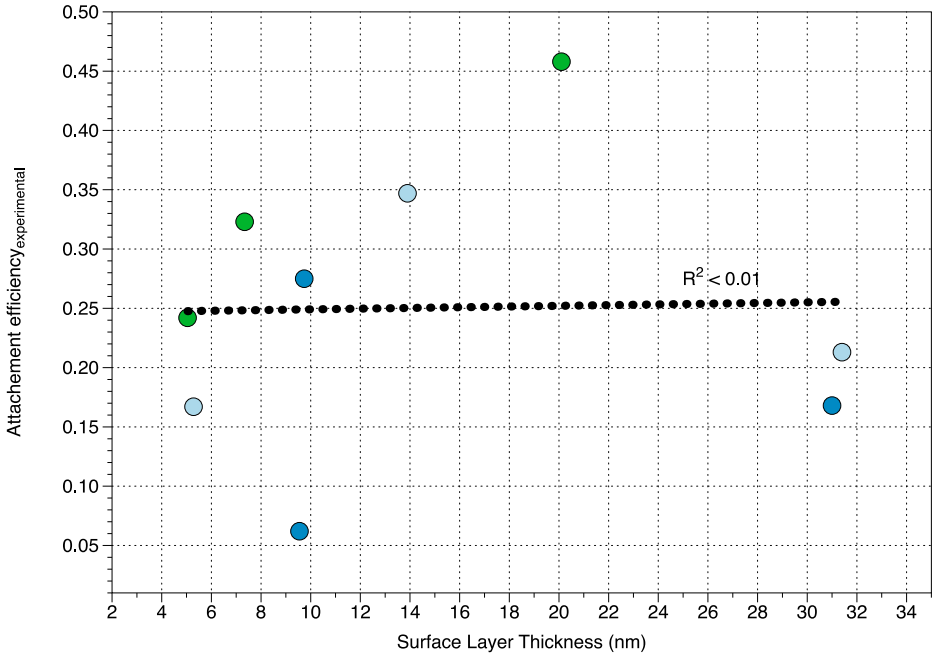

Fig. S8. Comparison of attachment efficiency calculated from column experiments with surface layer thickness for coatings. R^2 value of less than 0.01 indicates a very low correlation. Colours represent bare (white), humic acid- (light blue), PAA- (dark blue) and BSA-coated (green) particles.

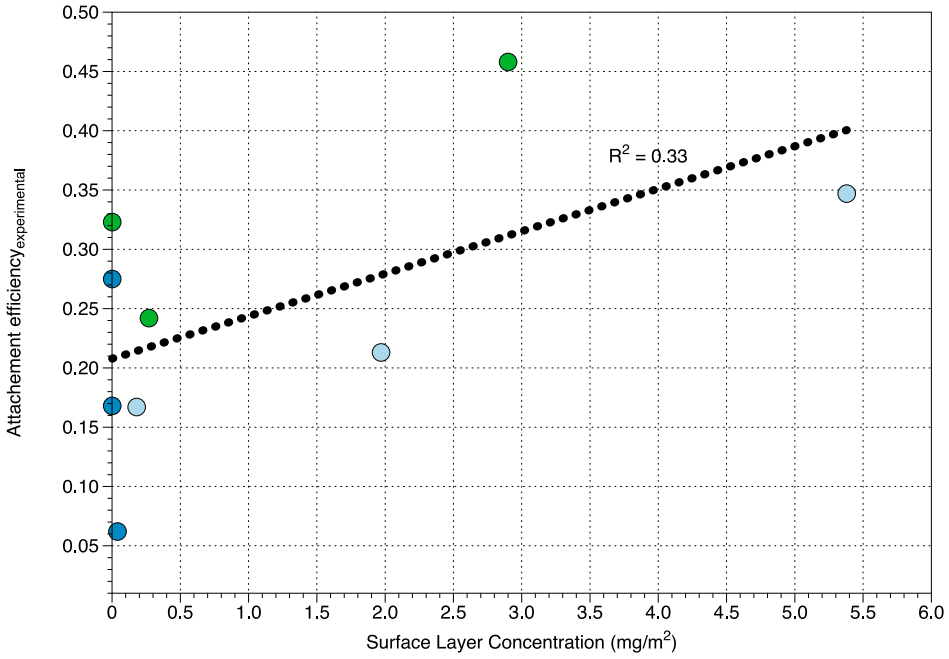

Fig. S9. Comparison of attachment efficiency calculated from column experiments with surface layer concentrations for coatings. R^2 value of 0.33 indicates minimal correlation. Colours represent bare (white), humic acid- (light blue), PAA- (dark blue) and BSA-coated (green) particles.

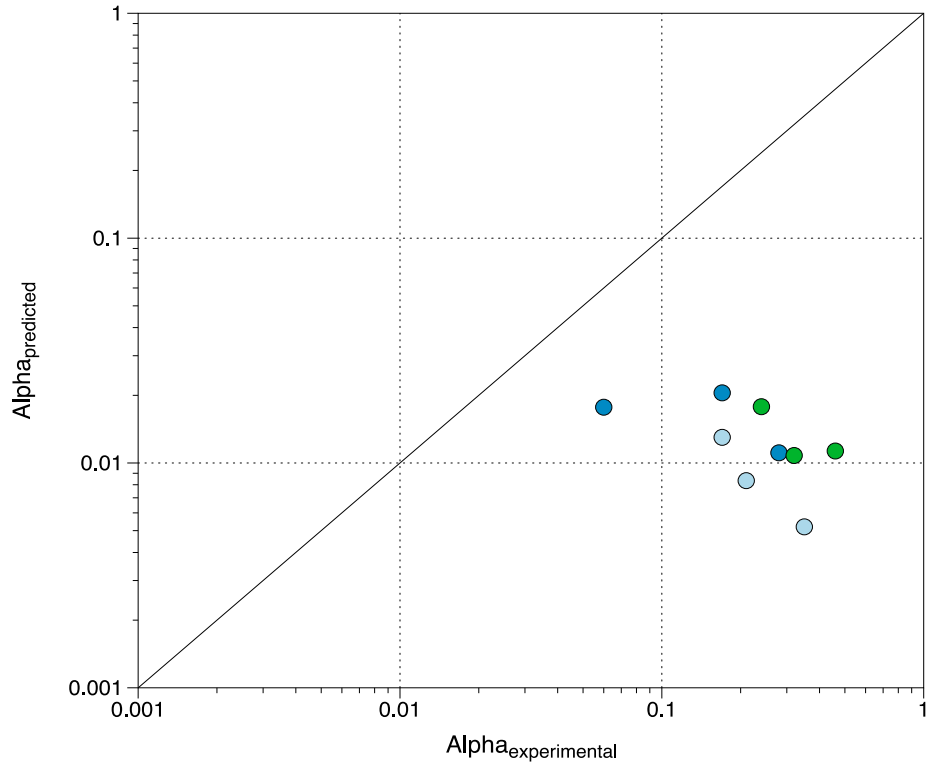

Fig. S10. Attachment efficiencies predicted from a semi-empirical correlation ($Alpha_{predicted}$) versus those experimentally determined in column experiments ($Alpha_{experimental}$). Colours represent bare (white), humic acid- (light blue), PAA- (dark blue) and BSA-coated (green) particles.

References

[1] J. E. Song, T. Phenrat, S. Marinakos, Y. Xiao, J. Liu, M. R. Wiesner, R. D. Tilton, G. V. Lowry, Hydrophobic interactions increase attachment of gum arabic- and PVP-coated Ag nanoparticles to hydrophobic surfaces. *Environ. Sci. Technol.* **2011**, *45*, 5988. doi:10.1021/es200547c

[2] K. Yang, D. H. Lin, B. S. Xing, Interactions of humic acid with nanosized inorganic oxides. *Langmuir* **2009**, *25*, 3571. doi:10.1021/la803701b

[3] R. Enriquez, P. Pichat, Interactions of humic acid, quinoline, and TiO_2 in water in relation to quinoline photocatalytic removal. *Langmuir* **2001**, *17*, 6132. doi:10.1021/la010599w

[4] J. Gao, K. Powers, Y. Wang, H. Y. Zhou, S. M. Roberts, B. M. Moudgil, B. Koopman, D. S. Barber, Influence of Suwannee River humic acid on particle properties and toxicity of silver nanoparticles. *Chemosphere* **2012**, *89*, 96. doi:10.1016/j.chemosphere.2012.04.024

[5] X. L. Wang, L. Shu, Y. Q. Wang, B. B. Xu, Y. C. Bai, S. Tao, B. S. Xing, Sorption of peat humic acids to multi-walled carbon nanotubes. *Environ. Sci. Technol.* **2011**, *45*, 9276. doi:10.1021/es202258q

[6] M. H. Li, C. P. Huang, Stability of oxidized single-walled carbon nanotubes in the presence of simple electrolytes and humic acid. *Carbon* **2010**, *48*, 4527. doi:10.1016/j.carbon.2010.08.032

[7] S. C. Liufu, H. N. Mao, Y. P. Li, Adsorption of poly(acrylic acid) onto the surface of titanium dioxide and the colloidal stability of aqueous suspension. *J. Colloid Interface Sci.* **2005**, *281*, 155. doi:10.1016/j.jcis.2004.08.075

[8] A. Foissy, A. E. Attar, J. M. Lamarche, Adsorption of polyacrylic acid on titanium dioxide. *J. Colloid Interface Sci.* **1983**, *96*, 275. doi:10.1016/0021-9797(83)90029-2

[9] S. Chibowski, M. Paszkiewicz, J. Patkowski, Adsorption of poly(acrylic acid) on the surface of TiO_2 in the presence of different surfactants. *Physicochem. Probl. Miner. Process.* **2012**, *48*, 317.

[10] T. Kopac, K. Bozgeyik, J. Yener, Effect of pH and temperature on the adsorption of bovine serum albumin onto titanium dioxide. *Colloid. Surface. A* **2008**, *322*, 19. doi:10.1016/j.colsurfa.2008.02.010

[11] C. E. Giacomelli, M. J. Avena, C. P. DePauli, Adsorption of bovine serum albumin onto TiO_2 particles. *J. Colloid Interface Sci.* **1997**, *188*, 387. doi:10.1006/jcis.1996.4750

[12] R. L. Williams, D. F. Williams, Albumin adsorption on metal-surfaces. *Biomaterials* **1988**, *9*, 206. doi:10.1016/0142-9612(88)90085-3

[13] J. W. Swan, E. M. Furst, A simpler expression for Henry's function describing the electrophoretic mobility of spherical colloids. *J. Colloid Interface Sci.* **2012**, *388*, 92. doi:10.1016/j.jcis.2012.08.026

[14] H. Ohshima, Electrophoresis of soft particles. *Adv. Colloid Interfac.* **1995**, *62*, 189. doi:10.1016/0001-8686(95)00279-Y

[15] J. F. L. Duval, H. Ohshima, Electrophoresis of diffuse soft particles. *Langmuir* **2006**, *22*, 3533. doi:10.1021/la0528293

[16] R. J. Hill, D. A. Saville, W. B. Russel, Electrophoresis of spherical polymer-coated colloidal particles. *J. Colloid Interface Sci.* **2003**, *258*, 56. doi:10.1016/S0021-9797(02)00043-7

[17] H. Ohshima, Electrophoretic mobility of a highly charged soft particle: relaxation effect. *Colloid. Surface. A* **2011**, *376*, 72. doi:10.1016/j.colsurfa.2010.09.012

[18] J. J. López-García, C. Grosse, J. Horno, Numerical study of colloidal suspensions of soft spherical particles using the network method – 1. DC electrophoretic mobility. *J. Colloid Interface Sci.* **2003**, *265*, 327. doi:10.1016/S0021-9797(03)00536-8

[19] T. Phenrat, N. Saleh, K. Sirk, H. J. Kim, R. D. Tilton, G. V. Lowry, Stabilization of aqueous nanoscale zerovalent iron dispersions by anionic polyelectrolytes: adsorbed anionic polyelectrolyte layer properties and their effect on aggregation and sedimentation. *J. Nanopart. Res.* **2008**, *10*, 795. doi:10.1007/s11051-007-9315-6

[20] T. L. Doane, C. H. Chuang, R. J. Hill, C. Burda, Nanoparticle zeta-potentials. *Acc. Chem. Res.* **2012**, *45*, 317. doi:10.1021/ar200113c

[21] T. Phenrat, J. E. Song, C. M. Cisneros, D. P. Schoenfelder, R. D. Tilton, G. V. Lowry, Estimating attachment of nano- and submicrometer-particles coated with organic macromolecules in porous media: development of an empirical model. *Environ. Sci. Technol.* **2010**, *44*, 4531. doi:10.1021/es903959c

[22] J. L. Viota, K. Rudzka, A. Trueba, I. Torres-Aleman, A. V. Delgado, Electrophoretic characterization of insulin growth factor (IGF-1) functionalized magnetic nanoparticles. *Langmuir* **2011**, *27*, 6426. doi:10.1021/la2009144

[23] S. M. Louie, T. Phenrat, M. J. Small, R. D. Tilton, G. V. Lowry, Parameter identifiability in application of soft particle electrokinetic theory to determine polymer and polyelectrolyte coating thicknesses on colloids. *Langmuir* **2012**, *28*, 10334. doi:10.1021/la301912j

[24] R. Brun, P. Reichert, H. R. Kunsch, Practical identifiability analysis of large environmental simulation models. *Water Resour. Res.* **2001**, *37*, 1015. doi:10.1029/2000WR900350

[25] N. Tufenkji, M. Elimelech, Correlation equation for predicting single-collector efficiency in physicochemical filtration in saturated porous media. *Environ. Sci. Technol.* **2004**, *38*, 529. doi:10.1021/es034049r